THE ASTROPHYSICAL JOURNAL, 340:29–46, 1989 May 1

THE CLUSTERING OF DWARF GALAXIES

JO ANN EDER
Yale University Observatory

JAMES M. SCHOMBERT
California Institute of Technology

AVISHAI DEKEL
The Hebrew University of Jerusalem

AND

AUGUSTUS OEMLER, JR.
Yale University Observatory

Received 1988 July 5; accepted 1988 September 30

ABSTRACT

We have studied the spatial distribution of dwarf irregular galaxies in and around a nearby void, as a test of some models of biased galaxy formation. New, deep Palomar Schmidt plates were searched for dwarf candidates in the vicinity of a void centered at $\alpha = 0^h45$, $\delta = +20°$, $v = 3500$ km s^{-1}. Velocities of 102 objects were obtained with the Arecibo[1] 305 m telescope. These proved to be typical dwarf irregulars, with average velocity widths of 100 km s^{-1} and absolute B-magnitudes of -16.0 (assuming $H_0 = 100$ km s^{-1} Mpc^{-1}). The distribution of the dwarfs is qualitatively similar to that of bright galaxies in the region, each set of objects equally well delineating voids and high-density regions. A quantitative analysis confirms this impression: except on small scales, where galaxy interactions may be depleting the numbers of very small dwarfs, the autocorrelation and cross-correlation functions, and the nearest-neighbor distributions of dwarfs and giants, are indistinguishable. We discuss the constraints that this result puts on specific models of biased galaxy formation.

Subject headings: cosmology — galaxies: clustering — galaxies: formation — galaxies: redshifts

I. INTRODUCTION

It is now clear that the distribution of galaxies in the universe contains very large structures, including lumps, sheets, and filaments. The existence of large voids is of particular relevance to some theoretical problems. Although the existence of regions of low density is predicted by all theories of galaxy clustering, there is evidence that at least some voids, including the one in Bootes (Kirshner *et al.* 1981) are too large and too empty to be consistent with the matter distribution predicted by any of the conventional theories, which assume gravitational growth of small-amplitude, Gaussian fluctuations (Kirshner *et al.* 1987). In such models, very large voids cannot be produced without violating the constraints on the clustering amplitude imposed by the isotropy of the microwave background and the galaxy autocorrelation function. If further observations show large voids to be a common occurrence, we will be faced with a choice between two options. It may be that a radically different theory of clustering is required, for example, one based on non-Gaussian fluctuations. Alternatively, bright galaxies, whose distribution defines the observed voids, may not be reliable tracers of the distribution of mass in the universe. This is the popular notion of biased galaxy formation (see Dekel and Rees 1987 for a review). It is attractive to many, not only as a means of reconciling various clustering models with the observed distribution of galaxies, but also because it removes the apparent discrepancy between the low value of the cosmic density parameter, Ω_0, deduced from observations and the value of unity predicted by inflationary models of the early universe.

If bright galaxies do not accurately trace the distribution of mass, voids in their distribution may be filled by other forms of matter. The possible forms are limited only by the imagination, but some alternatives seem more likely than others. The most conservative hypothesis suggests that, as environment changes, ordinary bright galaxies may be replaced by galaxies with somewhat different properties. A variety of arguments may be used to show why this might be so. White *et al.* (1987), elaborating on an argument by Kaiser (1984), have shown that, in cold dark matter (CDM) simulations, galaxies with deep potential wells, and therefore high internal velocities, are more clustered than those with shallow potential wells, and the latter are better tracers of the total mass distribution. Dekel and Silk (1986) have proposed a physical mechanism for galaxy biasing, based on the formation of diffuse dwarf galaxies through gas loss by supernova-driven winds. In this picture also, bright galaxies form only at highly clustered deep potential wells in the mass distribution, while gas-poor dwarf galaxies are distributed more like the matter. Although this theory is only directly relevant to dwarf ellipticals, Dekel and Silk have speculated that dwarf irregulars, which are much easier to observe, would have a similar distribution. In general, most theories of biasing invoke some physical process, to which protogalaxies of very different properties should have different sensitivity. Since the range from giant spirals, ellipticals, and S0 galaxies to faint dwarf irregulars spans most of the parameter space occupied by galaxies, one might expect dwarfs and giants to have observably different distributions as a result of most biasing processes.

[1] The Arecibo Observatory is part of the National Astronomy and Ionosphere Center, which is operated by Cornell University under contract with the National Science Foundation.

The observational evidence is ambiguous. Small-scale variations in galaxy populations, particularly around rich clusters, have been known for decades (Abell 1965; Oemler 1974; Davis and Geller 1976; Dressler 1980), but the possible relevance of these to galaxy biasing is not understood. Recently, Davis and Djorgovski (1985) have claimed that low surface brightness galaxies in the *Uppsala General Catalogue of Galaxies* (UGC; Nilson 1973) are distributed more smoothly than are those of high surface brightness, a phenomenon which they attribute to biasing. However, Bothun *et al.* (1986) have shown that this conclusion was due to the failure to account properly for differences in the selection of the two samples. Bothun *et al.*, using more homogeneous samples, show the two classes of galaxies to have qualitatively the same distributions. In any event, they point out that a large fraction of the low surface brightness UGC galaxies are not dwarfs but rather spirals of moderate to high luminosity. Even more recently, Thuan, Gott, and Schneider (1987) have shown that members of a sample of 58 galaxies classified as dwarf irregulars in the UGC lie in the same structures delineated by the bright galaxies of the CfA survey (Davis *et al.* 1982). There is no tendency for them to fill voids. Binggeli (1988) has found similar clustering in a large dwarf survey by Binggeli, Tarenghi, and Sandage (1988).

These results, while suggestive, are only qualitative. And, as White *et al.* (1987) have recently demonstrated, qualitative results may be misleading. In their model for a biased CDM universe, dwarfs and giants delineate the large-scale structure equally well. Only by applying quantitative measures such as the galaxy autocorrelation function can the effects of biasing be seen. Phillips and Shanks (1987) have indirectly estimated the relative correlation functions of bright and faint galaxies and have found them to be the same, but with large uncertainties. On the other hand, Giovanelli, Haynes, and Chincarini (1986) have determined the angular distribution of galaxies in the vicinity of the Pisces-Perseus Supercluster and find that irregulars are more smoothly distributed than earlier morphological types. Sharp, Jones, and Jones (1978) and White, Tully, and Davis (1988) have made similar claims for the distribution of dwarfs.

In this paper we describe another quantitative measurement of the relative distribution of dwarf and giant galaxies, in a region centered on a nearby void. We find that the two classes of galaxies have very similar distributions, a result which, if confirmed in larger studies, may cause difficulty for some theories of biasing. In § II we describe the sample and the observations made of it, and in § III the properties of the galaxies observed. In § IV we apply various tests to demonstrate the similarity of the distributions of the two types, and in § V we discuss the implications of this finding.

II. OBSERVATIONS

We wished to study a region containing a variety of structures, including lumps, sheets, and filaments, as well as voids. However, we wished to avoid rich clusters of galaxies, in which processes other than biased galaxy formation may have affected the relative numbers of dwarf and giant galaxies. Also, for the dwarfs to be easily observable from Arecibo, the region had to be at moderately positive declinations, and no more distant than about 5000 km s^{-1}. Several regions meeting these requirements could be identified from the distribution of galaxies in the CfA survey; for reasons of observing convenience, we have chosen one centered at $\alpha = 0^h45$, $\delta = +20°$, $v = 3500$ km s^{-1}. This region can be most clearly seen in Figures 5*a* and 5*b* of Davis *et al.* (1982); it appears roughly spherical, with a diameter of 1500 km s^{-1}.

From the field centers to be used in the Second Palomar Observatory Sky Survey (POSS; see Schombert and Bothun 1988), we have selected 15 which sample the void and the high-density regions which surround it. These are listed in Table 1, in which columns (1)–(3) give the Sky Survey field number and the coordinates (epoch 1950) of the field center. The location of the fields on the sky is presented in Figure 1. Also shown in Figure 1 (*filled circles*) are those CfA galaxies in the region with velocities between 2650 and 4150 km s^{-1}. These galaxies clearly delineate the void. Using the distribution of CfA galaxies, we have divided our 15 fields into two groups, designated ON or OFF void in column (4) of Table 1, indicating whether the field is or is not in the direction of the void. This designation is very approximate: some fields, particularly 476 and 611, span the boundary between the void and the surrounding high-density region.

As part of the preliminary work for the Second POSS, plates were obtained of all fields with the Palomar 48 inch (1.2 m) Schmidt telescope in the fall of 1985. All plates are on IIIa-J emulsion behind a GG 385 filter, and are 14 inches (35.6 cm) square, providing a usable field about 6°.3 across. Because the spacing of fields in the new POSS is 5°, there is significant overlap of adjacent fields. The plate quality is, in general, excellent, a significant improvement over earlier Palomar Schmidt plates obtained on coarse emulsions with the old corrector. Each plate was carefully inspected at least 3 times by eye, using a low-power magnifier. All objects which had diameters greater than about 20", and which were possible dwarf irregulars, were marked. These included all low surface brightness objects which were not obvious spirals, and a variety of irregularly shaped objects of higher surface brightness.

Regions around each object were scanned with the Yale PDS microdensitometer. Final classification of the objects was based on their appearance on the plates and on inspection of the scans using an image display system. Because of the distance and size of these objects, their classification is rather uncertain. Particularly among the more distant objects, there is an unavoidable tendency to misclassify late-type spirals as irregulars. Most of the candidates are of rather low surface brightness. Objects of higher than average surface brightness are subject to competing selection effects. They are easier to

TABLE 1
SECOND POSS FIELDS OBSERVED

Field	R.A. (1950)	Decl. (1950)	Void?
409..........	00^{h}00	+30°	OFF
474..........	00 44	+25	ON
475..........	01 06	+25	ON
476..........	01 28	+25	OFF
535..........	23 06	+25	OFF
538..........	00 00	+20	ON
539..........	00 21	+20	ON
540..........	00 42	+20	ON
541..........	01 03	+20	ON
609..........	00 40	+15	ON
611..........	01 20	+15	ON
681..........	00 40	+10	ON
685..........	02 00	+10	OFF
749..........	23 20	+10	OFF
822..........	23 40	+ 5	OFF

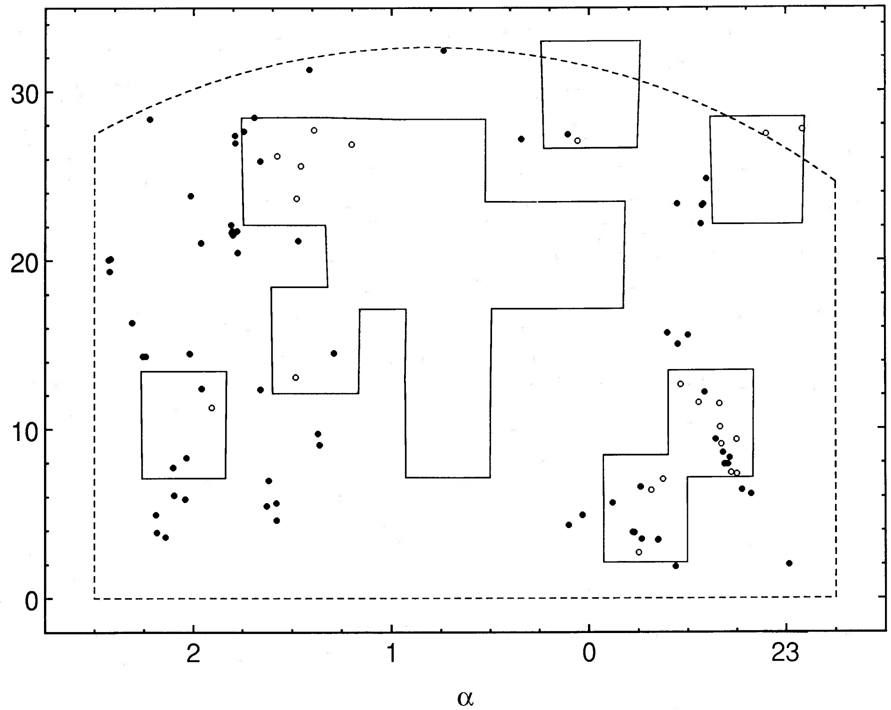

FIG. 1.—*Inner boxes*: area covered by the 15 POSS fields within which dwarfs were surveyed. *Outer, dashed box*: area of the CfA sample used in § IV*a*. *Filled circles*: location of CfA galaxies with velocities 2650 km s^{-1} < v < 4150 km s^{-1}. *Open circles*: location of dwarfs within the same velocity range.

find than low surface brightness ones, but, if spirals, they are less likely to be misclassified as irregulars. Because of the selection biases, which are variable and difficult to quantify, the galaxy sample is more reliably defined by its range of internal velocities than by what type of galaxy we were trying to find. In recognition of the uncertain classification, objects were given a numerical confidence class between 1 and 5, 1 indicating an object which had a high probability of being a dwarf irregular and 5 indicating an object which was very unlikely to be one. From the scans, the galaxy's position, its diameter at the lowest perceptible isophote, and its magnitude within that diameter were also measured. The magnitudes are less than optimum, being based on an approximate characteristic curve for the plates. There are 23 objects in common between our set of galaxies and those in the *Catalog of Galaxies and Clusters of Galaxies* (Zwicky *et al.* 1961–1968, hereafter CGCG). Because we have no photoelectric photometry of our galaxies, we have set the zero point of our magnitude scale by comparison with the Zwicky photometry.

We observed 132 of the galaxies in our list at 21 cm with the Arecibo 305 m telescope in 1986 May and June. All observations were made with the 21 cm dual-circular feed positioned to provide a maximum gain (8 K Jy^{-1}) at 1400 MHz. We were fortunate to be able to use the new 2048 channel autocorrelator with a baseline response much improved over the old 1008 channel autocorrelator. The independent, oppositely polarized signals were each divided into two subcorrelators of 512 channels. In order to search a larger velocity space, the secondary local oscillators of each polarization set of subcorrelators were offset on either side of the standard local oscillator frequency of 260 MHz by 8.75 MHz, allowing a total velocity coverage of 8000 km s^{-1}, a velocity resolution of 8.6 km s^{-1}, and some overlap at the band edges. The observations were centered on 4000 km s^{-1}, which avoided detection of the strong Galactic hydrogen signal on the low-velocity end, and extended to 8120 km s^{-1}. Observations were made in the total power mode with 5 minute ON-source and OFF-source observations. In most cases, only one 5 minute ON-source integration was required for detection. Wherever possible, the zenith angle was kept less than 14° to minimize the degradation of the gain. The reference noise sources and the zenith angle and broad-band feed responses were calibrated with standard radio continuum sources from the catalog of Bridle *et al.* (1972) and from the Bonn compilation (Kuhr *et al.* 1981). In order to assure ourselves that the system and the data reduction system were stable, each day we observed several bright galaxies with well-determined 21 cm spectra (Lewis, Helou, and Salpeter 1985).

The GALPAK data reduction program, developed by R. Giovanelli and M. Haynes, was used to obtain the H I spectral parameters for each detected galaxy. Frequency and zenith-angle gain corrections were applied to each (ON − OFF)/OFF spectrum, and the two polarizations were combined. The resulting spectra for the two velocity ranges were then smoothed with a three-channel boxcar function followed by a Hanning function. The smoothing increased the average total signal-to-noise ratio of the spectra to 15, and the velocity resolution to 20 km s^{-1}. A polynomial (generally of order 3 or less) was fitted to the baseline and then subtracted before the systemic velocity, the velocity width, and the integrated flux were measured. No correction for beam dilution was necessary, since all of the galaxies had diameters much less than the half-power beamwidth. For a more detailed discussion of the feed characteristics and the data reduction, the reader is referred to Haynes and Giovanelli (1984) and Bicay and Giovanelli (1986).

Radio interference spikes were quite common in our spectra, and some galaxies had spectral profiles so narrow that they were difficult to distinguish from interference at the resolution which our observations produced. To assure ourselves that the signals did indeed originate in the galaxies, we reobserved most of the narrow profiles ($\Delta v < 40$ km s^{-1}) using a resolution of 1.1 km s^{-1}. The autocorrelator was reconfigured to provide one subcorrelator of 1024 channels for each polarization. The observations were made in the frequency-switching mode with ON and OFF frequencies equally spaced above and below the frequency of the observed peak. This technique produced spectra with the galaxy signal in both the ON and the OFF spectra. The OFF signal was inverted, shifted, and averaged with the ON signal. All of these high-resolution spectra displayed typical galaxy profiles, half with steep edges and an indication of double peaks, and half with Gaussian shapes.

The object list, divided by Sky Survey field, is presented in Table 2. Unless we obtained radio observations of them, objects with measured diameters less than 24″ were eliminated from the final list, because it was clear that the original list was seriously incomplete for smaller objects. The incompleteness for larger objects is very difficult to estimate, dependent as it is on the surface brightness, magnitude, and morphology of the galaxies in addition to their angular size. The contents of Table 2 are as follows: Column (1) gives POSS field number. Columns (2) and (3) give the galaxy coordinates (epoch 1950), accurate to about 10″. Column (4) lists other catalog designations of the object. Column (5) gives the *B* magnitude, on the CGCG scale, within the diameter listed, and column (6) the diameter in arcseconds. For irregularly shaped objects, this size is the longest dimension. Column (7) gives a surface brightness description, "high," "medium," or "low." Column (8) gives the confidence class. In column (9) the heliocentric velocity is given, defined as the midpoint of the profile above a level 50% of the peak flux. When no other H I properties are listed for the galaxy, the CfA optical velocity is given. Column (10) gives the velocity corrected for the motion of the Sun relative to the center of mass of the Local Group, according to the precepts of de Vaucouleurs, de Vaucouleurs, and Corwin (1976). Column (11) gives the velocity width, at 50% of maximum. Given in column (12) is the total flux, in mJy km s^{-1}. Comments are given in column (13). These are, for the most part, self-explanatory. Those designated as "interacting" are irregularly shaped objects which may be interacting pairs of galaxies.

Where three dots appear in columns (9)–(12) the objects were observed but undetected; where there are blanks, the objects were not observed. Objects whose radio parameters are in parentheses were marginal detections. Also included are previous observations: these are cited in the "Comments" column. We checked each detected galaxy on our plates for other nearby galaxies that might have been within the Arecibo beam or its sidelobes when the beam was centered on the program galaxy. Any possible sources of confusion are mentioned in the notes. The spectra, and all 21 cm data not pertinent to this paper, will be presented in a later paper (Eder and Oemler 1989).

In the radio observations, preference was given to those galaxies with diameters greater than 25″ and confidence classes less than 4. However, because one is constrained, at Arecibo, to a narrow range of right ascension at any one time, we were not able to obtain observations that were totally complete to any particular limit. Some galaxies in our preferred range of parameters were missed, while we observed a few galaxies smaller than 24″ in diameter, and a few from confidence classes 4 and 5. Our final list contains 178 galaxies. Of the objects in classes 1–3, we observed (but did not necessarily detect) 40% of those with diameters of 24″, 70% of those with diameters between 27″ and 40″, and 95% of the larger objects. Out of 132 galaxies observed in the radio, we obtained 98 detections and four marginal detections. Thirty galaxies were not detected in 5 (or, at most, 10) minutes of integration time.

III. GALAXY PROPERTIES

Tests of the quality of our optical data are limited to comparisons with the data in the CGCG and the UGC, to multiple observations of five galaxies in regions of overlap between adjacent plates, and to a second reduction of the PDS scans of one field, using a different characteristic curve and independent estimates of the sizes of the galaxies. From all of these checks, we estimate the accuracy of our photometry to be about 0.2 mag. The limiting factor is the difficulty in defining the "total" magnitude of a galaxy using aperture measurements. We estimate that the zero point of our photometry has been set to the scale of the CGCG to an accuracy of about 0.1 mag.

In Figure 2*a* we compare our measured diameters with those of the same galaxies determined by Nilson (1973). Several things are apparent from this plot. First, the scatter is fairly small, indicating that it is possible to measure galaxy diameters reliably by eye. This is consistent with our internal checks, which suggest a repeatability in our diameter measurements of about 10%. Second, our sizes are consistently smaller than those of Nilson, by about 20%. An inspection of some galaxy images on the original POSS, which Nilson used, indicates that our definition of size is somewhat more conservative than his. Nevertheless, given the superior quality of the plates of the new Sky Survey, and the fact that we have measured the objects using an image display, which allowed us to enhance the contrast of the images considerably, we were rather surprised that we were not able to see much fainter isophotes than Nilson could. Another surprise, apparent from Figure 2*b*, is that we discovered very few galaxies with diameters greater than 1′

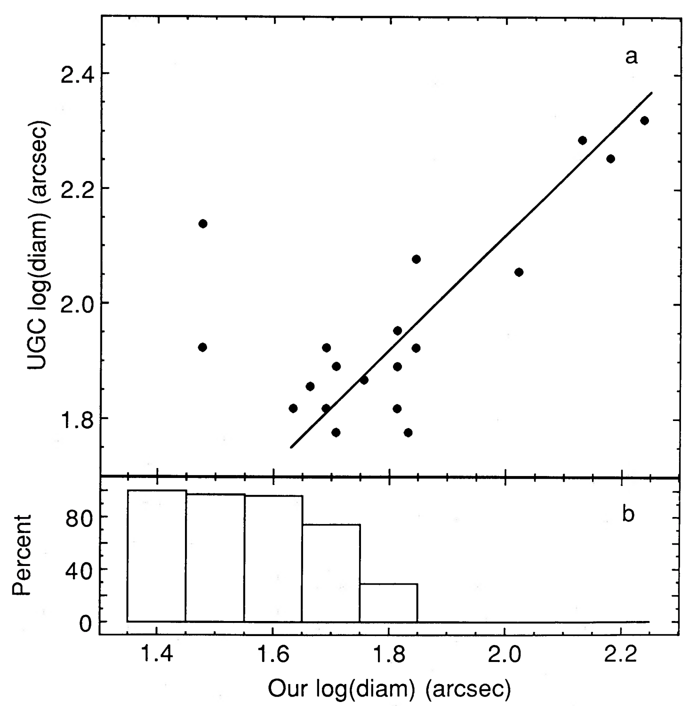

FIG. 2.—(*a*) Comparison of our measured diameters with those of the UGC. (*b*) Percentage of our dwarf sample missing from the UGC vs. our diameter.

TABLE 2

THE GALAXY SAMPLE

Field (1)	R. A. (2)	Dec. (3)	Name (4)	mB (5)	Diam (arcsec) (6)	S.B. (7)	Conf (8)	V_h (km sec^{-1}) (9)	V_o (km sec^{-1}) (10)	ΔV (km sec^{-1}) (11)	$\int S_v dv$ (mJy km sec^{-1}) (12)	Comments (13)
409	00 00 22.2	+29 18 21		18.1	41	L	2	4836	5074	114	1400	
409	00 02 00.5	+31 26 10		16.1	41	M	3					Irr/Merg
409	00 02 04.9	+29 19 14		16.8	35	L	2					
409	00 03 28.4	+27 04 17		16.3	49	L	1	3181	3412	69	1500	
409	00 04 52.7	+31 47 39		17.2	46	L	3	4864	5105	100	2100	Interacting?
409	00 07 29.4	+27 57 04		17.0	24	L	3					
409	00 11 41.3	+28 37 10		16.6	41	L	3	7060	7291	167	1800	Nucleated
409	00 12 36.0	+28 58 18		17.7	35	L	1	6899	7130	62	330	
409	00 12 56.3	+28 22 44		17.4	27	L	2	6682	6911	87	930	
409	00 13 21.4	+27 12 05		17.4	27	L	3	...	...	...	...	Spec??
409	00 13 49.5	+27 17 54		17.1	14	L	2	4597	4823	92	870	
409	23 48 05.0	+28 40 36		17.4	30	L	2	...	...	...	...	
409	23 48 41.0	+32 42 43		16.7	32	M	3	4951	5202	128	940	Spec?
409	23 57 11.5	+26 58 38		17.6	30	L	2	4699	4934	64	890	
474	00 32 21.5	+24 34 54		18.3	24.	L	2	5480	5689	121	610	Spiral??
474	00 35 05.7	+23 56 00		18.3	24.	L	2	4650	4855	103	750	
474	00 36 39.6	+24 27 18		16.1	38	M	3					Dist Spiral??
474	00 41 18.1	+25 52 25		17.2	30	L	3	4898	5105	38	950	
474	00 43 22.9	+27 31 08		18.0	24	L	3					
474	00 45 36.1	+26 11 42		16.1	30	H	3					
474	00 47 31.3	+26 57 08		18.2	24	L	3					
474	00 47 55.3	+26 33 45		19.0	27	L	2	...	...	...	...	
474	00 52 54.7	+23 55 29		17.6	35	L	2	4980	5174	82	1300	2 Spec?
474	00 54 03.1	+22 51 25		16.9	27	L	3	...	...	...	...	
475	00 54 39.0	+23 37 12	UGC591/Mk350	15.0	51	H	4	5260	5260			Strbrst?
475	00 55 46.5	+23 32 37		17.1	30	L	3	...	...	...	...	Disk
475	01 01 46.0	+22 13 30		17.7	32	L	3	5662	5845	118	1200	
475	01 12 01.2	+26 52 23		15.5	46	L	2	3618	3807	111	4900	Spiral?
476	01 19 47.4	+26 56 28		16.7	46	L	3	...	...	...	...	Spiral??
476	01 21 18.1	+26 47 15	UGC948	17.1	43	L	3	4908	5091	163	2800	(1)
476	01 23 22.4	+27 42 31		17.4	38	L	3	4021	4205	75	1100	Double (2)
476	01 27 22.2	+25 36 28	UGC1073	14.8	105	L	2	3678	3678	152	9300	(3)
476	01 28 37.2	+23 41 49	UGC1084	17.1	49	L	2	3414	3582	65	4400	(4)
476	01 34 28.5	+26 10 57		18.0	27	L	2	3872	4044	66	990	
476	01 35 27.8	+22 25 32		17.5	38	L	3	...	...	...	...	Sm?
476	01 39 29.3	+26 06 57		16.9	32	M	2	359	527	38	1100	
476	01 40 09.0	+27 18 48		18.0	24	L	2					
476	01 41 16.3	+24 37 01		18.2	24	L	3					
535	22 54 57.9	+27 42 42		17.4	49	L	2	2944	3207	108	2400	Pec
535	22 56 36.1	+26 09 07		16.9	24	L	3	7705	7964	65	840	Spiral???
535	22 57 02.6	+24 51 32		19.1	19	L	1	7417	7673	75	730	
535	23 01 14.7	+23 24 59		16.4	35	L	2	1155	1406	94	2700	
535	23 03 54.6	+27 37 13		17.9	24	L	2	6913	7173	68	530	
535	23 05 52.2	+27 26 47		16.2	54	L	2	2884	3143	86	2900	Pec

1989ApJ...340...29E

TABLE 2—*Continued*

Field (1)	R. A. (2)	Dec. (3)	Name (4)	m_B (5)	Diam (arcsec) (6)	S.B. (7)	Conf (8)	V_h (km sec^{-1}) (9)	V_o (km sec^{-1}) (10)	ΔV (km sec^{-1}) (11)	$\int S_v dv$ (mJy km sec^{-1}) (12)	Comments (13)
535	23 07 09.1	+26 33 25		17.6	35	L	1	...	...	...	...	
535	23 16 51.8	+24 39 37		16.9	41	L	1	5809	6057	94	1500	
535	23 19 13.4	+27 23 16		16.6	27	L	2	5935	6188	45	940	Interacting?
538	00 00 14.4	+18 41 22		17.0	41	M	3	713	924	50	1100	
538	00 01 56.8	+20 26 20		16.6	30	M	3					
538	00 02 13.0	+18 01 56		17.2	30	L	3	6315	6523	77	1000	Interacting?
538	00 03 25.9	+21 35 06		17.1	24	L	3					SB?
538	00 04 06.9	+21 06 05		17.9	24	L	2	...	...	...	...	
538	00 05 57.4	+17 53 04		15.8	30	H	3					
538	00 08 39.5	+22 55 54		16.8	27	M	2					Irr
538	00 09 20.0	+20 54 42		16.2	30	M	3					
538	00 09 47.5	+17 31 09		16.9	24	M	3					
538	00 10 08.1	+20 36 50		15.8	35	M	3					
538	00 10 21.1	+18 15 43		17.6	32	L	1	5514	5718	32	490	Dwarf
538	00 11 18.3	+23 03 33		16.5	27	M	2					Irr?
538	23 47 32.6	+21 29 50		17.4	24	L	3	...	...	...	...	
538	23 48 10.3	+19 31 13		17.6	24	L	1	...	...	...	...	Dwarf
538	23 52 56.9	+17 38 29	UGC12843	13.7	151	M	4	1769	1981	150	15000	(5)
538	23 53 12.9	+18 08 53	UGC12846	15.4	70	L	1	1739	1953	94	6200	(6)
538	23 57 06.6	+17 21 37		16.9	35	L	3	6457	6666	174	1200	
538	23 59 03.9	+17 12 38		17.9	35	L	3	6413	6621	72	850	
539	00 14 28.9	+22 43 11		16.1	51	L	3	4405	4619	118	2200	Irr/Merg
539	00 14 40.6	+17 14 50	UGC159	17.4	30	L	1	1005	1204	72	2200	
539	00 14 44.1	+20 31 36		15.9	54	L	3	4366	4574	144	5000	
539	00 16 13.7	+19 42 45		17.0	38	L	1	5542	5747	72	1400	
539	00 18 05.3	+22 18 55		14.7	46	H	4	7352	7563	197	3500	Merg? (7)
539	00 18 22.7	+17 24 47	UGC200	16.4	49	L	1	5235	5432	136	1500	(8)
539	00 20 30.4	+20 22 56		16.7	24	M	3					
539	00 21 52.2	+20 46 42		18.4	27	M	3	5246	5451	76	580	Ring?
540	00 29 58.9	+22 18 17		18.1	32	L	3	4560	4764	118	1100	SB?
540	00 38 04.7	+22 24 06		17.1	30	L	2	5899	6098	73	660	2 Spec? (9)
540	00 43 33.6	+19 12 21	UGC477	15.2	173	M	5	2646	2832	231	18000	(10)
540	00 44 17.8	+21 18 18		16.7	41	L	2	5180	5372	72	1200	Spiral?
540	00 46 14.8	+20 03 20		17.7	30	L	3	...	...	...	...	Interacting?
540	00 46 56.6	+19 47 06		18.1	35	L	2	...	...	...	...	
540	00 51 17.3	+20 07 19		15.5	32	H	3					
540	00 54 04.3	+22 50 08		17.6	24	L	2					
540	00 54 40.2	+19 08 10		16.3	32	H	3					
541	00 58 02.6	+20 53 50		16.9	27	M	3					
541	00 58 11.5	+18 10 28		16.8	24	L	3					
541	01 03 30.5	+18 01 07		16.7	27	L	3					Nucleated
541	01 05 59.6	+21 15 29		16.6	32	L	2	5546	5723	100	1700	
541	01 06 06.5	+17 13 33		17.1	24	L	3					

TABLE 2—*Continued*

Field (1)	R. A. (2)	Dec. (3)	Name (4)	m_B (5)	Diam (arcsec) (6)	S.B. (7)	Conf (8)	V_h (km sec^{-1}) (9)	V_o (km sec^{-1}) (10)	ΔV (km sec^{-1}) (11)	$\int S_v dv$ (mJy km sec^{-1}) (12)	Comments (13)
609	00 35 24.6	+13 47 23		18.7	30	L	1	...	...	...	...	
609	00 35 45.3	+13 12 20		16.8	35	L	3	5597	5770	102	660	(11)
609	00 35 48.3	+13 12 44	UGC385	15.7	30	M	4	5459	5632	158	1600	Interacting? (11)
609	00 42 17.2	+16 39 57	UGC472	15.5	65	L	3					Spiral??
609	00 52 10.2	+13 23 25		17.0	43	L	1	5428	5590	66	1300	
611	01 08 17.4	+17 43 35		17.0	27	M	3					
611	01 08 27.5	+17 41 09		16.9	30	M	3	...	...	...	...	
611	01 15 08.1	+17 11 35		16.8	46	L	3	...	...	...	...	Sm?
611	01 15 11.2	+13 14 39		16.3	35	M	3					Interacting?
611	01 17 06.5	+16 31 48		16.9	35	L	1	2163	2318	32	1200	
611	01 18 23.7	+16 48 44	UGC883	15.4	57	L	3					Sm?
611	01 18 38.9	+12 09 02	UGC891	14.9	135	L	2	644	783	103	12000	(12)
611	01 20 19.1	+17 12 17		16.2	27	M	3					Spiral??
611	01 20 32.4	+12 02 18		18.1	24	L	2	(4869)	(5006)	(105)		(13)
611	01 20 38.9	+17 01 43		16.2	35	M	2					
611	01 22 35.0	+13 53 52		17.9	43	L	1	5041	5183	35	1200	
611	01 23 49.4	+16 58 20		15.9	35	M	3					
611	01 24 32.9	+13 20 36	UGC1026	15.9	70	L	1	4505	4643	102	2500	(14)
611	01 26 06.4	+16 25 55	UGC1056	14.7	51	M	3	594	742	49	2200	
611	01 27 25.5	+13 20 31		16.6	41	L	3	6395	6531	120	1800	
611	01 27 34.8	+14 25 11		16.8	43	L	1	2449	2589	121	3800	
611	01 28 55.9	+13 04 29		16.6	38	L	2	2739	2873	107	820	
611	01 29 05.9	+13 53 54		16.1	57	L	3	6763	6900	175	2300	Sm?
611	01 29 23.8	+12 29 59		16.2	30	H	3					Strbrst?
611	01 29 59.7	+18 03 28	UGC1104	14.4	46	H	3					
611	01 31 25.1	+12 35 01		16.5	27	L	2	5019	5149	104	860	
681	00 28 59.6	+08 53 42		20.4	32	L	2	2156	2319	108	5900	
681	00 33 40.1	+09 31 11		17.3	38	L	1	...	...	...	...	
681	00 37 44.2	+08 36 10		16.5	35	M	3	5249	5405	138	2100	
681	00 40 02.0	+09 43 50		18.0	24	L	1	5071	5229	63	460	(15)
681	00 40 35.6	+08 32 56		17.2	35	L	2	5363	5517	110	660	
681	00 47 14.8	+10 19 54		17.6	27	L	1	...	...	...	...	
681	00 47 22.2	+08 54 21		17.1	32	M	3	...	...	...	...	
681	00 48 22.4	+07 25 43		18.8	24	L	2					
685	01 48 01.1	+11 54 34		17.7	51	L	3	6873	6988	166	1900	(16)
685	01 48 16.2	+09 53 07		17.7	30	M	3	...	...	...	...	
685	01 48 23.6	+10 24 30		18.5	24	L	2	...	...	...	...	
685	01 49 06.0	+11 39 19		16.9	49	L	3	4839	4952	188	4600	Sm?
685	01 49 46.7	+11 18 33		17.4	24	M	2	...	...	...	...	
685	01 50 49.2	+12 34 51		17.9	30	M	2	4656	4771	84	630	
685	01 52 06.7	+10 19 08		16.5	68	L	1	6085	6191	37	2200	
685	01 52 20.7	+10 36 41		17.2	38	M	3	6205	6312	193	1600	(17)
685	01 52 41.2	+10 05 05		17.4	32	L	3	...	...	...	...	Spiral??
685	01 53 57.3	+09 55 12		18.6	27	L	1	6135	6238	65	1100	
685	01 54 27.1	+11 17 12		15.9	46	M	3	3470	3578	112	2800	

1989ApJ...340...29E

TABLE 2—*Continued*

Field (1)	R. A. (2)	Dec. (3)	Name (4)	m_B (5)	Diam (arcsec) (6)	S.B. (7)	Conf (8)	V_h (km sec^{-1}) (9)	V_o (km sec^{-1}) (10)	ΔV (km sec^{-1}) (11)	$\int S_v dv$ (mJy km sec^{-1}) (12)	Comments (13)
685	01 55 30.9	+09 44 09		18.2	30	L	3	5888	5989	169	1300	(18)
685	01 55 48.1	+07 08 26		18.8	27	L	1	...	...	...	...	
685	01 57 02.8	+10 10 32		18.7	30	L	1	6302	6403	77	1100	
685	01 57 03.4	+12 02 51		17.8	38	L	1	7828	7936	145	1500	
685	01 58 22.0	+08 15 24		20.1	38	L	1	7804	7897	147	1900	
685	01 59 10.1	+12 38 37		17.8	27	M	3	...	...	...	...	
685	01 59 19.6	+11 29 22	UGC1515	17.0	51	M	4	4643	4747	136	1200	Sdm?
685	02 00 09.4	+07 34 32		19.1	41	L	1	(5771)	(5860)	(159)	(1000)	(19)
685	02 05 50.3	+12 06 08		18.1	24	L	3					
685	02 09 40.8	+12 58 17		17.6	27	M	3	(2262)	(2363)	(156)	(800)	(20)
685	02 12 22.4	+08 35 53		16.8	35	M	3	1590	1673	38	1000	
749	23 07 07.1	+12 23 46		16.6	30	L	2	...	...	...	...	
749	23 08 35.7	+11 05 40		15.8	38	L	2	2639	2853	69	1500	Sm?
749	23 10 11.8	+10 27 29	Mk526	14.7	173	H	5	6579	6790	129	1700	
749	23 10 17.4	+12 13 22		16.0	35	L	3	4891	5108	142	1800	Spiral?
749	23 13 06.3	+07 02 28		15.4	41	H	3					Merger?
749	23 14 55.1	+07 21 39	UGC12480	15.5	68	L	2	3872	4071	91	3500	(21)
749	23 15 04.3	+09 22 54		16.3	51	L	2	3811	4016	127	1400	
749	23 15 17.4	+11 09 05		16.4	30	L	2					
749	23 16 25.2	+07 30 21		17.3	27	L	3	4310	4508	102	820	
749	23 16 38.7	+07 25 50	UGC12497	15.2	65	L	2	3762	3960	159	3600	
749	23 16 39.2	+09 44 49		16.4	30	L	1					
749	23 19 41.4	+09 06 32	UGC12553	15.3	70	L	2	3574	3776	83	2700	(22)
749	23 20 05.4	+10 06 35		17.0	30	L	1	3521	3727	127	1700	
749	23 20 15.5	+11 29 54	UGC12562	15.3	65	L	3	3836	4046	154	2000	(23)
749	23 26 39.9	+11 34 28		16.0	49	L	1	3648	3855	76	1800	
749	23 31 10.8	+08 58 43		16.2	35	L	3					Nucleated
749	23 32 11.3	+12 39 09		16.8	27	L	1	3838	4046	119	1200	
822	23 29 46.8	+03 30 41		16.3	41	M	5					
822	23 32 52.6	+05 46 01		17.3	35	M	2	...	...	...	...	Sm? (24)
822	23 36 32.2	+07 32 09		15.9	41	M	3					Interacting?
822	23 36 41.6	+04 08 00		17.0	35	M	3	6400	6576	161	1400	Interacting?
822	23 36 50.7	+04 05 07		17.3	30	M	3	...	...	...	...	Interacting?
822	23 37 36.1	+07 01 53		17.6	49	L	1	3699	3885	92	2600	
822	23 38 40.1	+05 38 49		17.0	32	L	2	1732	1913	86	1700	
822	23 39 20.9	+02 41 55		18.3	30	L	3	...	...	...	...	Spiral??
822	23 41 08.9	+06 24 02		17.8	38	L	3	3809	3991	138	1000	Spiral??(25)
822	23 42 50.4	+06 33 15		17.7	41	L	2	5308	5490	84	1700	
822	23 42 59.8	+06 08 13		18.5	24	L	2					
822	23 44 17.4	+06 34 56		16.4	49	L	2	(3050)	(3231)	(70)	(1500)	(26)
822	23 44 55.1	+02 42 28		18.2	27	L	2	3808	3975	65	1200	
822	23 46 46.8	+03 54 12		18.6	24	L	2	2971	3141	73	570	
822	23 47 31.5	+05 21 48		17.6	22	L	3					Spiral??
822	23 47 48.1	+06 54 35		17.1	27	M	3	...	...	...	...	
822	23 48 11.6	+03 42 27		17.9	35	L	1					
822	23 51 36.4	+03 37 42		17.8								

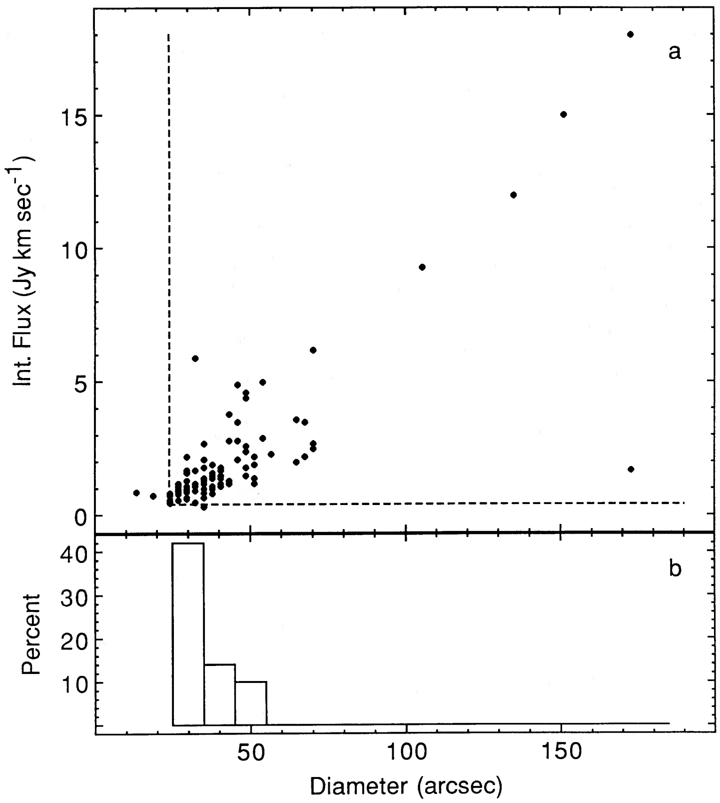

FIG. 3.—(*a*) Integrated H I flux vs. angular diameter of the dwarf sample. (*b*) Percentage of galaxies undetected at 21 cm vs. diameter.

which had been missed by Nilson. Schombert and Bothun (1988) have already discussed the latter fact, and have concluded that the abundance of extremely low surface brightness galaxies is rather small. Another effect, which must be of some importance, is the deterioration of the sky at Palomar during the 30 years since the original POSS, due primarily to the growth of San Diego. Our plates would be particularly sensitive to this increase in sky brightness, since all of the fields are in the south.

We may judge the accuracy of our 21 cm observations by repeat observations, and by comparison with published data. We made 13 observations of seven galaxies from the list of Lewis, Helou, and Salpeter (1985). Our measured velocities for these galaxies differed from the published values by less than 1 km s^{-1}, in the mean, with a standard deviation of individual measurements of 6 km s^{-1}. For the velocity widths, the corresponding numbers are -5 and 6 km s^{-1}. The small systematic difference in velocity width may be due to the use of slightly different measuring algorithms, but, in any event, the differences are within the observational errors expected for our measurements. Our sample of galaxies also contained 10 already observed by Giovanelli and Haynes (1985, 1988) or Giovanelli *et al.* (1986) (we shall hereafter refer to these three papers collectively as GH). The mean and standard deviation of the velocity differences were respectively -4 and 5 km s^{-1}, and of differences in the velocity widths -5 and 9 km s^{-1}, again well within the observational uncertainties. We observed six galaxies more than once. The standard deviations of the velocities and velocity widths between pairs were respectively 4 and 2 km s^{-1}.

Of the 132 objects observed, 30 were not detected. It is of interest to know whether this was because their hydrogen emission was too weak or because they were outside the observable velocity range of 120–8120 km s^{-1}. A possible answer is given by Figures 3*a* and 3*b*, which plot the integrated 21 cm flux of the detected galaxies and the fraction of undetected

NOTES TO TABLE 2.—(1) V_h = 4918 km s^{-1} (Giovanelli *et al.* 1986). (2) The spectral profile is a single peak, but a pair of galaxies are centered in the telescope beam. (3) V_h = 3675 km s^{-1} (Giovanelli *et al.* 1986). (4) V_h = 3414 km s^{-1} (Giovanelli *et al.* 1986). (5) V_h = 1777 km s^{-1} (Giovanelli and Haynes 1988). (6) V_h = 1744 km s^{-1} (Giovanelli and Haynes 1988). (7) The spectral profile appears to be that of two systems. (8) V_h = 5234 km s^{-1} (Giovanelli and Haynes 1988). (9) Interference at the edge of the signal makes the H I properties uncertain. (10) V_h = 2657 km s^{-1} (Giovanelli and Haynes 1988). (11) Objects 003545.3+131220 and 003548.3+131244 (UGC 385) are interacting. The spectral profile has been deconvolved by eye to provide the velocity, velocity width, and integrated flux of the two systems, but the assignment of hydrogen peak to optical galaxy may be reversed. Giovanelli and Haynes 1988 report V_h = 5512 km s^{-1} for UGC 385. (12) V_h = 646 km s^{-1} (Giovanelli and Haynes 1988). (13) Very marginal 4 detection. (14) V_h = 4513 km s^{-1} (Giovanelli and Haynes 1988). (15) Two possible signals are in the OFF beam. They could be two galaxies seen on the plates at 004627.9+092834 and at 004615.4+092813. These were not included in our sample because they have a confidence rating of 5. (16) A poor baseline causes measured quantities, other than the central velocity, to be uncertain. (17) There may be another object in the beam with V_h = 4910 km s^{-1}, ΔV = 91 km s^{-1}, and $\int S\,dv$ = 580 mJy km s^{-1}. No visible optical source for this signal is seen on the plate, however. (18) The spectral profile is suggestive of two close galaxies, but only one is visible on the plate. (19) Interference within the profile make the H I measurements uncertain. (20) Extremely marginal detection. (21) V_h = 3870 km s^{-1} (Giovanelli and Haynes 1988). (22) V_h = 3572 km s^{-1} (Giovanelli and Haynes 1988). (23) V_h = 3834 km s^{-1} (Giovanelli and Haynes 1988). (24) Possible detection at V_h = 475 km s^{-1}. (25) Marginal detection. (26) UGC 12778 is also within the beam with V_h = 3296 km s^{-1} as compared with V_h = 3298 km s^{-1} measured by Giovanelli and Haynes 1988.

galaxies against their angular diameter. The correlation in Figure 3*a* is quite good, indicating, as is well known (Haynes and Giovanelli 1984), that most galaxies of one morphological type have roughly the same hydrogen surface density. Our detection limit depends on velocity width, narrow-lined galaxies being more easily detected than those with very broad hydrogen velocity profiles. However, from typical values of velocity width (100 km s^{-1}) and noise per channel (1.5 mJy), we estimate the average detection limit for our dwarfs to be about 500 mJy km s^{-1}. It is apparent, then, from Figure 3, that most of the missing galaxies were not detected because their hydrogen flux was too weak to be detected. Although this does introduce a bias toward high hydrogen content into our velocity sample, its effect is probably less important than that of the dominant one: our sample consists only of those galaxies which looked, to one observer (A. O.), like dwarf irregulars.

In Figure 4 we present the distribution of velocity widths of our galaxies, and also of those late-type galaxies in the Virgo Cluster cataloged by Binggeli, Sandage, and Tammann (1985, hereafter BST) and observed at 21 cm by Hoffman *et al.* (1987). It appears that we were successful in selecting dwarf irregulars, and that our confidence class is a useful measure of the reliability of our classification. Galaxies with confidence values of 1 and 2 have velocity widths like the BST Im III's, those in class 3 are similar to the Sdm's and Sm's, while those in classes 4 and 5 have the larger widths characteristic of earlier spirals. The absolute blue magnitudes of the galaxies, as a function of recessional velocity, are presented in Figure 5, subdivided by confidence class. Again, it is apparent that confidence class is a useful measure of our success in selecting low-luminosity galaxies: those of class 4 and 5 are significantly more luminous than the others. The shallow trend of absolute magnitude with recessional velocity is due to the poor correlation of brightness with angular size, which was the selection criterion of the sample. However, because size is well correlated with hydrogen flux, there is a slightly stronger variation of hydrogen mass with recessional velocity, as demonstrated in Figure 6.

Finally, we should comment on the optical surface brightness of our galaxies. It must be stressed that a calculation of mean surface brightness using the magnitudes and sizes in Table 2 can be very misleading. The angular size quoted is the longest dimension of the system. Some of the class 4 and 5 objects are probably interacting spirals, and a few have long tidal tails. The total surface area of these objects is much less than $\pi(d/2)^2$. The surface brightness description in column (7) of Table 2 is a more reliable, though a cruder, measure. From a subset of UGC galaxies in our sample, we find that the mean blue surface brightness of objects which we denoted as of high, medium, and low surface brightness is, respectively, 23.5, 24.8, and 26.4 mag arcsec^{-2}.

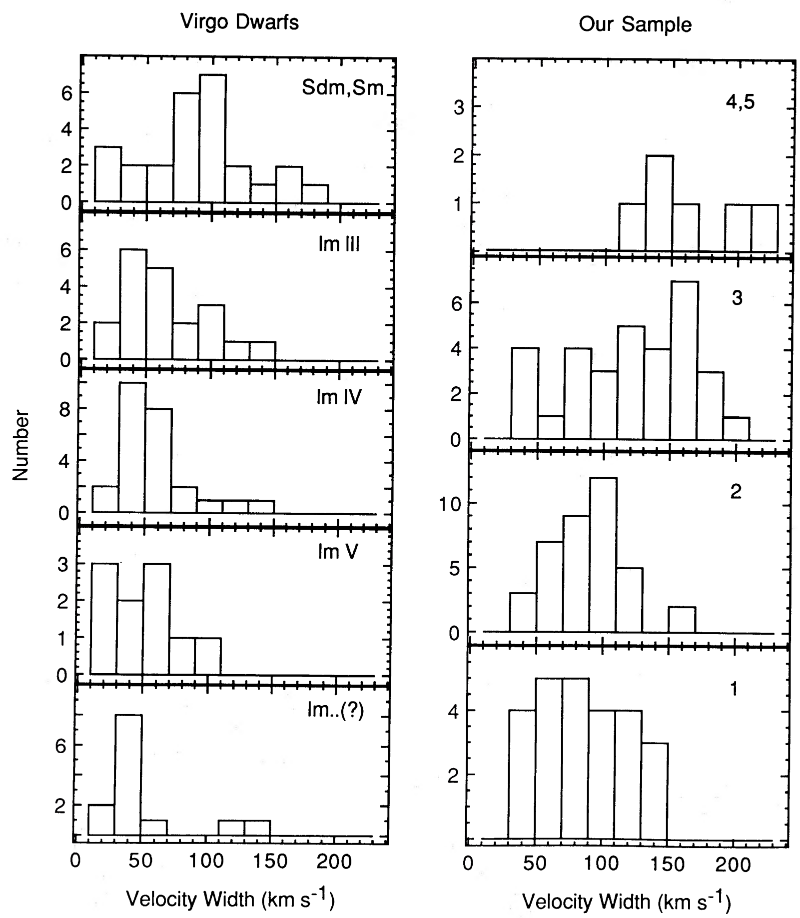

FIG. 4.—Distribution of H I velocity widths of the Virgo dwarfs observed by Hoffman *et al.* (1987) and those reported in this paper. The Virgo dwarfs are subdivided by morphological class, our dwarfs by confidence class.

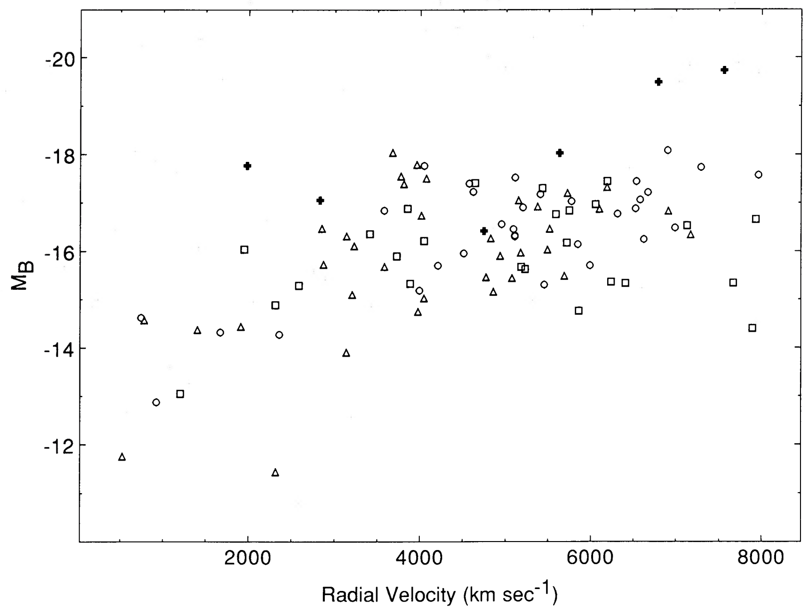

FIG. 5.—Absolute blue magnitudes of our dwarfs vs. their recessional velocity. *Circles*: dwarfs of confidence class 1; *triangles*: class 2; *squares*: class 3; *heavy plus signs*: classes 4 and 5.

IV. SPACE DISTRIBUTION OF THE DWARFS

We shall compare the space distribution of our dwarf galaxies with those of two samples of bright galaxies. One sample consists of all galaxies in the CfA survey within the limits $\delta > 0°$, $b < -30°$, $22^h45 < \alpha < 2^h30$. These limits are shown in Figure 1 as dashed lines. They encompass the entire region containing our survey fields except for parts of fields SS 409 and SS 535, which are at lower Galactic latitudes than the limit of the CfA catalog. This sample should be a fair representation of the distribution of bright galaxies within our survey area. The other sample, hereafter denoted the GH sample, consists of those galaxies within the limits of our 15 survey fields which are contained in the GH 21 cm survey. Parts of this survey remain to be published; Drs. Giovanelli and Haynes have very generously given us access to these data in order to complete our sample. The space density of GH galaxies is higher than that of galaxies in the CfA survey, but this sample is limited, of necessity, to later-type galaxies with a significant H I content. In Figure 7 we compare the distribution of observed velocity widths of the dwarf and GH samples. It is apparent that the GH galaxies are, on average, much more massive than the dwarfs.

A first, qualitative look at the relative distributions of the dwarf and CfA giant galaxies in our survey volume is presented in Figure 8. It is apparent that the void is as well delineated by

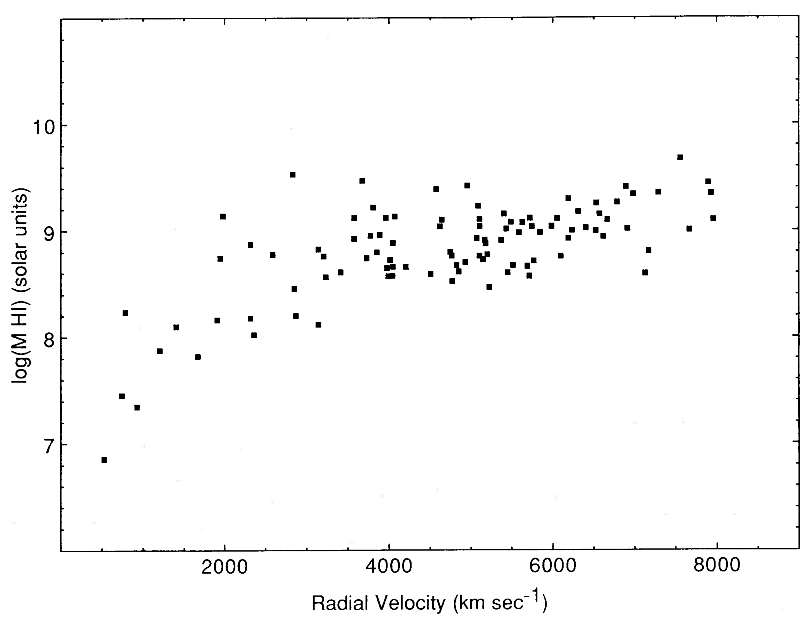

FIG. 6.—Hydrogen mass (calculated assuming $H_0 = 100$ km s^{-1} Mpc^{-1}) of the dwarfs vs. recessional velocity

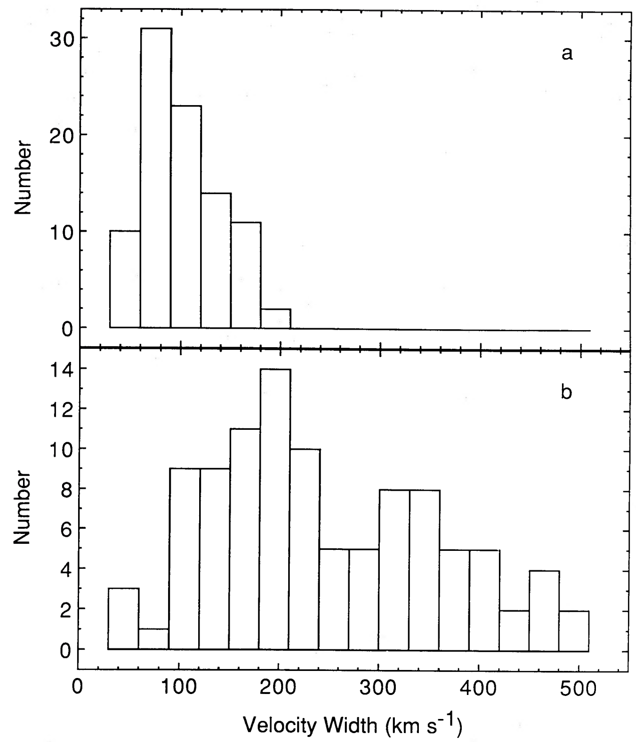

FIG. 7.—Distribution of observed hydrogen velocity widths of (*a*) our dwarf sample and (*b*) the GH giant sample.

the dwarfs as by the giant galaxies. A slightly more quantitative comparison is presented in Figure 9. Using the distribution of CfA galaxies in this region, we have divided our 15 fields into two groups. One group, containing those fields whose line of sight penetrates the void, are designated "ON-void" fields in Table 1. The other group contains the remaining "OFF-void" fields. In Figure 9 we present the distribution of radial velocities of the GH sample, and of our dwarf sample, in the two groups of fields. The radial distributions of the dwarfs and the GH giants are strikingly similar. With the exception of one galaxy, located at $\alpha = 1^h12^m1^s.2$, $\delta = +26°52'23''$, $v = 3604$ km s^{-1} in SS 475, the dwarfs faithfully delineate the same low- and high-density regions defined by the GH galaxies. When viewed in three dimensions, it is clear that the one apparent exception is not unusually isolated. It is about $9h^{-1}$ Mpc from the nearest CfA galaxy, which, as we shall demonstrate in § IV*b*, is not abnormal. Also shown in Figure 9, by smooth curves, are the velocity distributions expected if the galaxies were homogeneously distributed. These curves have been calculated from the selection functions and intrinsic galaxy properties in a way which is described below. It is apparent that the relative overdensities and underdensities of the dwarf and GH samples are very similar throughout the survey volume.

This similarity is suggestive, but, as mentioned earlier, is not sufficient as a test of galaxy biasing. We shall, therefore, calculate three statistics of the distributions of the three samples: the spatial autocorrelation function of galaxies within one sample, the spatial cross-correlation function between the members of two samples, and the nearest-neighbor distributions. The autocorrelation function is probably the most sensitive test. However, the small size of the dwarf galaxy sample and the peculiar shape of the sample volume limit the number of close pairs expected and give a result of rather low statistical weight.

Our analysis of the galaxy correlation functions is based on the discussion in Kirshner, Oemler, and Schechter (1979, hereafter KOS). We define the autocorrelation function $\xi(r)$ as

$$1 + \xi(r) = \sum \rho(r)/\rho'(r) , \qquad (1)$$

where $\rho(r)$ is the density of galaxies at distance r from a galaxy, $\rho'(r)$ is the expected density if galaxies were homogeneously distributed, and the sum is over all galaxies in the sample. The definition of the cross-correlation function is the same, except that $\rho(r)$ is the density of galaxies in sample 2 at a distance r from a galaxy in sample 1, and the sum is over all galaxies in sample 1. For magnitude-limited samples, this definition is preferable to another commonly used one,

$$1 + \xi(r) = N(r)/N'(r) , \qquad (2)$$

where the N's are the observed and expected numbers of pairs of separation r, because equation (2) produces a result heavily weighted toward the nearest part of the survey volume, where the density of sample objects is highest. We shall assume that the radial distance of each galaxy is exactly proportional to its

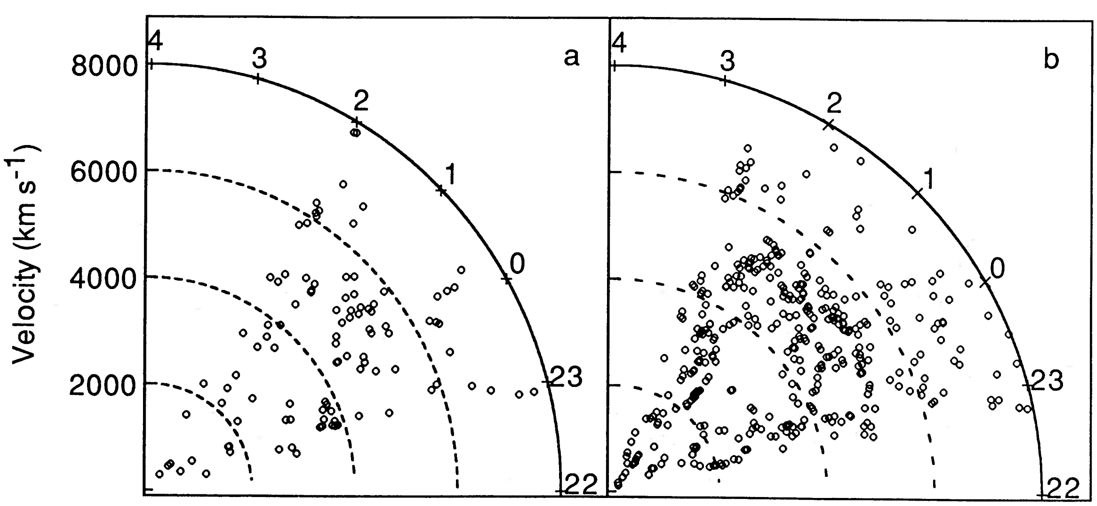

FIG. 8.—Distribution in the right ascension–heliocentric velocity plane of galaxies in (*a*) our dwarf sample and (*b*) the CfA sample

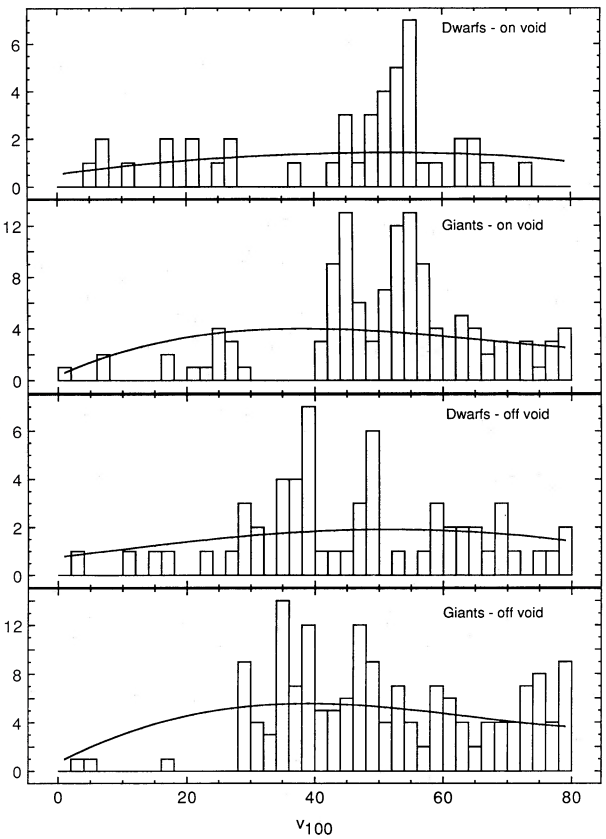

FIG. 9.—Velocity distribution of the dwarfs and GH giants, divided into those in "ON void" and "OFF void" fields according to the classification in Table 1. The smooth curves are the predicted velocity distributions if the galaxies were of uniform space density.

recessional velocity. Although a poor assumption at small velocity separations, where departures from pure Hubble flow are undoubtedly important, the effect of this on the results should be the same for the dwarf and giant samples.

Either equation requires knowledge of the expected density of objects in a homogeneous distribution. To estimate this properly, the sample must have been selected in a well-defined way, and one must know the intrinsic distribution of the parameter used in the selection. For example, analysis of an apparent-magnitude–limited sample requires knowledge of the magnitude limit and of the intrinsic luminosity function of the objects. These conditions are met by the CfA sample, and are almost met by our dwarf sample. The CfA sample is limited to apparent magnitudes brighter than 14.5, and its luminosity function has been determined by Davis and Huchra (1982). From this we calculate the expected density distribution in the manner described by KOS.

From our dwarf sample we can construct a subset, limited to objects with angular diameters $\theta \geq 24''$ and confidence classes ≤ 3. This sample of 168 objects is not complete: 74 have no measured velocities, because they were unobserved (46) or undetected (28). However, if these represent a random subset of the objects of their angular size, as they probably do, this incompleteness can be easily accounted for. Since the selection parameter for our sample is diameter, we need to know the intrinsic diameter function of the dwarfs. This may be constructed in a way analogous to that used to obtain luminosity functions. There exist techniques (see KOS) for constructing the latter which make no assumption about the space distribution of the objects, but these methods only work well for larger samples than we have available. We shall, therefore, use the conventional method, based on an assumed uniform density distribution. Although obviously incorrect, its effect on the derived diameter function should be fairly small, and on the derived correlation function much smaller still. A second estimate of the dwarf diameter function can be derived from the almost volume-limited sample of Virgo dwarfs produced by BST. For this we have used galaxies classified as types Sd, Sm, and Im, and intermediate types. Both results are presented in Figure 10, where we have shifted the scale of the BST data by -0.15 in the log, to account for a systematic difference in the diameter scales which we have established by comparing our diameters with those in the UGC, and the UGC diameters with those of BST. The agreement of the two determinations is good. The form of the diameter function is similar to that of luminosity functions, and can be fitted to a Schechter function

$$\varphi(D)\,dD = \varphi^* \exp\,[-(D/D^*)^2](D/D^*)^{-1}\,d(D/D^*)\,, \qquad (3)$$

where $D^* = 10.2h^{-1}$ kpc.

The definition of our third sample, that of GH, is more complex, with both magnitude and diameter limits, and we could not calculate the expected density distribution in the same way. Instead, we have taken the velocity distribution of all published GH galaxies, which cover an area much larger than that of our survey, and smoothed it to remove small-scale irregularities. The resulting distribution is not dissimilar to that which one would expect for a homogeneous density distribution, and should work reasonably well.

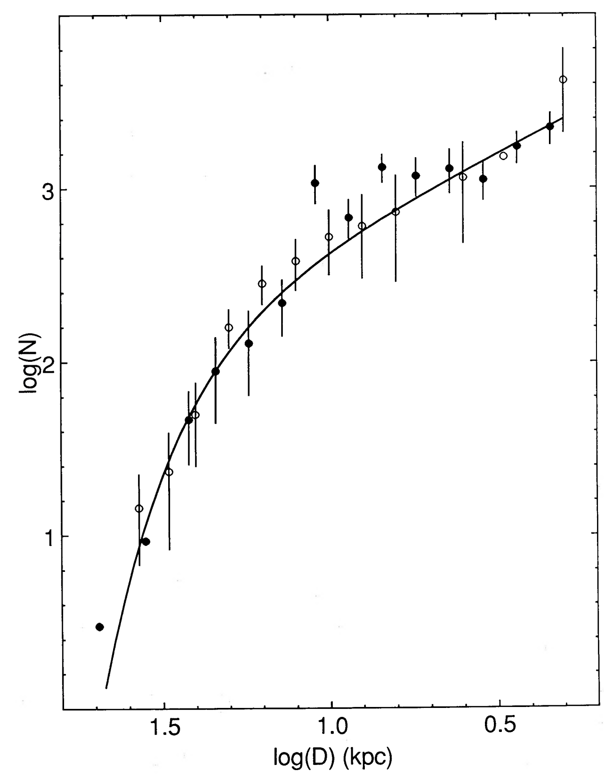

FIG. 10.—Diameter function of dwarf galaxies. *Open circles*: Virgo dwarfs, shifted in log r by -0.15; *filled circles*: dwarfs from this paper. *Solid line*: fit of eq. (3) to the data.

a) *The Correlation Functions*

We first calculate the autocorrelation function of the CfA sample. We limit the sample to the region of the sky described above, and to velocities in the range 1000 km s^{-1} < v < 8000 km s^{-1}. The result is presented in Figure 11*a*. The straight line, which is of the usual form, $\xi(r) = (r/r_0)^{-1.8}$, fits the data well. The amplitude is, however, quite small, with a correlation length, r_0, of 3.2h^{-1} Mpc. This is even smaller than the value of 4.5h^{-1} Mpc derived from the CfA sample by Davis and Peebles (1983), and much smaller than the value of 8h^{-1} Mpc, which Kirshner *et al.* (1989) have determined to be the best fit to all extant data. This discrepancy need not, however, alarm us. As Kirshner *et al.* demonstrate, derived values of r_0 fluctuate widely from sample to sample, presumably because of large-scale variations in the clustering of galaxies. The small region which we have selected for study is simply one with less than average clustering power. This is hardly surprising, since we have deliberately chosen a region devoid of rich clusters. (Voids make little contribution to the correlation function, unless they fill a much larger fraction of the sample volume than does ours.)

We now calculate the cross-correlation function of the GH and dwarf galaxies within our 15 survey fields against the CfA galaxies within the volume defined earlier. For this, we use velocity limits for the GH and dwarf galaxies of 1000–8000 km s^{-1} and for the CfA galaxies of 0–10,000 km s^{-1}. In Figures 11*b*–11*e* we present the results for, respectively, the GH giants, all the dwarfs, and the dwarfs subdivided into those with velocity widths greater than and less than 100 km s^{-1}. Finally, in Figure 11*f* we present the dwarf galaxy autocorrelation function. On each plot is superposed the power-law fit to the CfA data. We have not attempted to calculate the uncertainty of the points in these functions. The formal errors due to pair statistics are, typically, very small (smaller than the circles in Fig. 11). However, the true errors are undoubtedly much larger, and are dominated by unknown volume-to-volume variations in the clustering properties.

b) *Nearest-Neighbor Statistics*

The distribution of the distances from galaxies to their nearest neighbors is another measure of small-scale galaxy clustering, which is complementary to the correlation function. The correlation function is most sensitive to dense clumps in the galaxy distribution, while the nearest-neighbor distribution is sensitive to voids. If the dwarfs tend to fill voids, they should, on average, have more distant nearest neighbors than the giants. Unfortunately, the calculation of nearest-neighbor distributions is less straightforward than that of correlation functions. Unlike the latter, which are independent of the density of sample galaxies, the nearest-neighbor distributions are sensi-

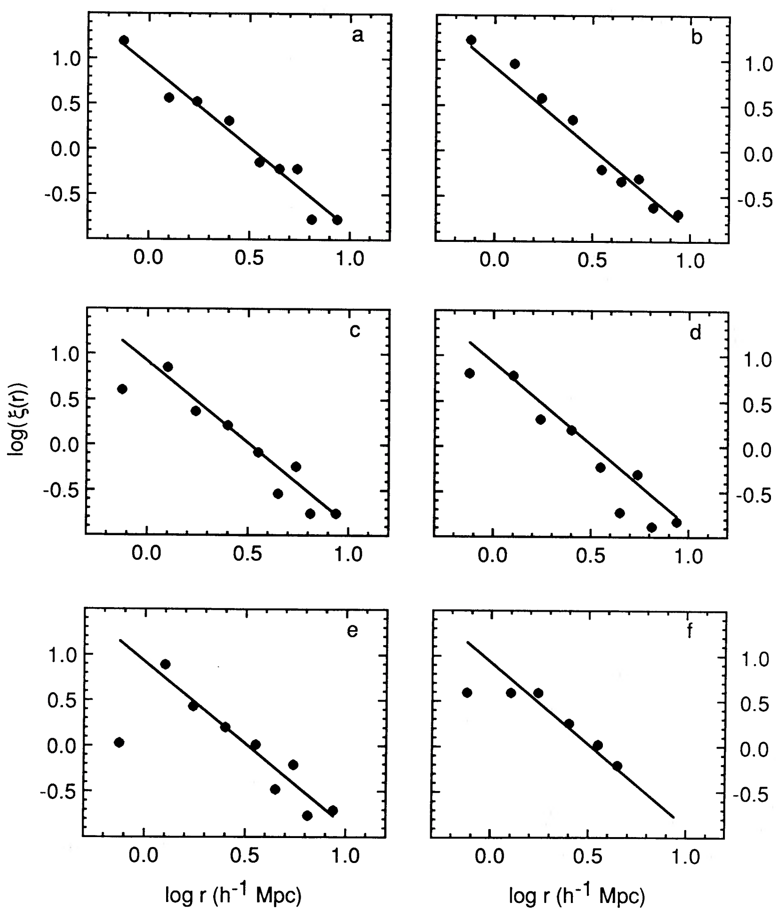

FIG. 11.—Correlation functions of the galaxy samples. (*a*) Autocorrelation function of the CfA sample. (*b*) GH vs. CfA cross-correlation function. (*c*) Dwarf vs. CfA cross-correlation function. (*d*) High-mass (δv > 100 km s^{-1}) dwarf vs. CfA cross-correlation function. (*e*) Low-mass (δv < 100 km s^{-1}) vs. CfA cross-correlation function. (*f*) Dwarf autocorrelation function.

tive to galaxy density, and in a way which is dependent on the details of the galaxy clustering.

We wish to calculate the distance from members of the GH and dwarf sample to the nearest CfA galaxy. The space density of CfA galaxies varies rapidly with distance, owing to the apparent magnitude limit of the sample. Thus low-velocity GH and dwarf galaxies will have much closer nearest neighbors than those at higher velocities. We could still compare the total distributions for the two samples, *if* those samples had the same radial velocity distributions, since they would then contain the same proportion of galaxies sampling each density of CfA objects. Since they do not, we have corrected the samples by the following procedure. We have limited both samples to the range 2000 km $s^{-1} < v <$ 6000 km s^{-1} in order to minimize the density range of the CfA galaxies. All of the dwarf galaxies were used. From the GH sample, we have calculated at each radial velocity the relative overabundance of GH galaxies, compared with that of dwarfs, and have randomly selected a subset small enough to give the two samples the same radial distributions. The result is presented in Figure 12, which plots the fraction of galaxies in each sample with nearest neighbors of a particular distance.

V. DISCUSSION

The results presented in the previous section are rather clear. With one exception, the distributions of all samples are identical. The exception is the innermost ($\langle r \rangle = 0.75h^{-1}$ Mpc) points of the correlation functions, which are significantly lower in all of the dwarf samples. A comparison of Figures 11*d* and 11*e* suggests that this effect is due almost entirely to the smaller dwarfs. Although this could be the result of some biasing process, the fact that its effect is only apparent at small separations suggests that it may be due to galaxy-galaxy interactions. Low-mass irregulars are probably not very robust objects, and might be easily disrupted if too close to other galaxies. (The Magellanic Clouds could be offered as a counterexample to this hypothesis. However, the Clouds may be the remnant of a once larger group of dwarf satellites; and the interactions of which the Magellanic Stream is evidence suggest that the Clouds' long-term prognosis is not good.)

Beyond $1h^{-1}$ Mpc, the distributions are indistinguishable in slope and amplitude, implying that dwarf irregulars are distributed no more smoothly than other, more massive galaxy types. This is consistent with most, but not all, of the work cited in § I. Giovanelli, Haynes, and Chincarini (1986, hereafter GHC), found a steadily decreasing clustering amplitude of UGC galaxies in the vicinity of the Pisces-Perseus Supercluster, as one progressed along the Hubble sequence from ellipticals through spirals to irregulars. This variation is primarily a manifestation of the well-known morphology-density relation (Dressler 1980), which is probably the result of galaxy interactions rather than biased galaxy formation (Oemler 1988). However, the large difference which GHC deduce between the clustering properties of spirals and irregulars is inconsistent with the results of this paper.

It is possible that the GHC results are, like those of Davis and Djorgovski (1985), an artifact of their use of the angular distribution of galaxies on the sky as a measure of clustering. The angular distributions of two samples can be meaningfully compared only if the samples have the same distribution along the line of sight. Since irregulars are, on average, much fainter than spirals, one would expect a much larger fraction of them to be in the foreground of the Pisces-Perseus Supercluster, which, at a velocity of 5000 km s^{-1}, provides most of the clustering power in this region. Examination of the velocity data presented in GH confirms this expection: foreground contamination is 5 times higher among the irregulars than among the entire sample. To further complicate things, Thuan, Gott, and Schneider (1987) have pointed out that few of the more distant UGC irregulars are, in fact dwarfs: most are of high luminosity, even though they are low surface brightness objects.

A more serious conflict is provided by the papers of Sharp, Jones, and Jones (1978, hereafter SJJ) and White, Tully, and

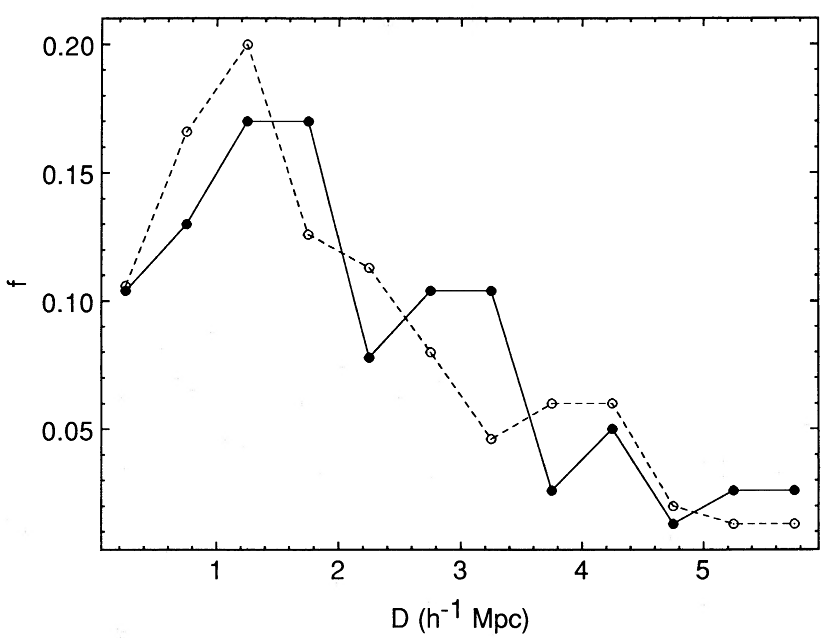

FIG. 12.—Distribution of distances from galaxies to the nearest CfA galaxy. *Filled circles*: dwarf sample. *Open circles*: GH sample.

Davis (1988, hereafter WTD). SJJ have calculated the angular cross-correlation function of luminous galaxies in the CGCG with a sample of dwarf irregulars studied by Fisher and Tully (1975). They find the dwarfs to be more weakly correlated with the luminous galaxies than the latter are with themselves, suggesting that the dwarfs are less clustered. WTD have examined the spatial distribution of galaxies in the *Nearby Galaxies Catalog* (Tully 1988). This catalog is claimed to be substantially complete for galaxies with $M_B < -16.0$ (assuming $H_0 = 75$ km s^{-1} Mpc^{-1}), out to the distance of the Virgo Cluster, and includes an estimate of the density of galaxies in the neighborhood of each catalog member. The Fisher-Tully dwarfs constitute a substantial fraction of the dwarfs in this sample. WTD assign to each galaxy a circular velocity, v_c, based either on direct observations or on empirical mean relationships between v_c and absolute magnitude. Galaxies with recessional velocities of less than 2250 km s^{-1} are divided into four intervals of v_c, and the distribution of neighborhood densities determined for members of each v_c group. They find a strong dependence of density on v_c: massive, high-v_c galaxies are much more concentrated toward high-density regions than are low-mass systems.

These results seem to contradict our findings directly, but there are some problems with the samples used in both studies. WTD point out that much of the difference between the density distributions of the four v_c groups is due to galaxies in a few rich clusters, primarily Virgo and Fornax. The same is likely to be true of the SJJ sample. An analysis of the Virgo members, which dominate this subset, is presented in Figure 13. The histogram shows the distribution of apparent magnitudes of all galaxies in the BST Virgo sample which those authors judged to be cluster members. The hatched area of the histogram includes that fraction of this sample which are known to be cluster members on the basis of their radial velocities, measured in the CfA survey. The heavily shaded area represents that fraction of the BST sample which is included in the *Nearby Galaxies Catalog*. The vertical dashed line is at the claimed limit of substantial completeness of that sample. Brackets at the top show the correspondence between apparent magnitude and the four v_c groups used by WTD. Obviously, the sample of fainter galaxies is very incomplete—about 90% incomplete in the lowest velocity group. We have also compared the Tully sample with the CfA catalog in a shell of distance comparable to Virgo, but excluding the region of the cluster itself. That comparison indicates that the incompleteness of the entire sample, while serious, is much less than that in Virgo, perhaps reaching 50% in the lowest velocity group.

It is clear that the galaxy sample in the *Nearby Galaxies Catalog* is systematically biased against dwarf galaxies in high-density regions. Since the Fisher-Tully sample used by SJJ is a subset of this, it is undoubtedly biased also. The explanation is quite straightforward. Most of the redshifts of the dwarf galaxies come from 21 cm observations. Dwarf galaxies in clusters are more likely to be gas-poor dE's, for which 21 cm observations cannot be made. It is very likely that the effect found by SJJ and WTD is simply an artifact of the incompleteness of the samples. (Because of the bias against faint ellipticals, there is another systematic bias in the sample. WTD's highest velocity group contains 90% E's and S0's; the lowest velocity group contains 1% E/S0's. Thus any residual segregation left after

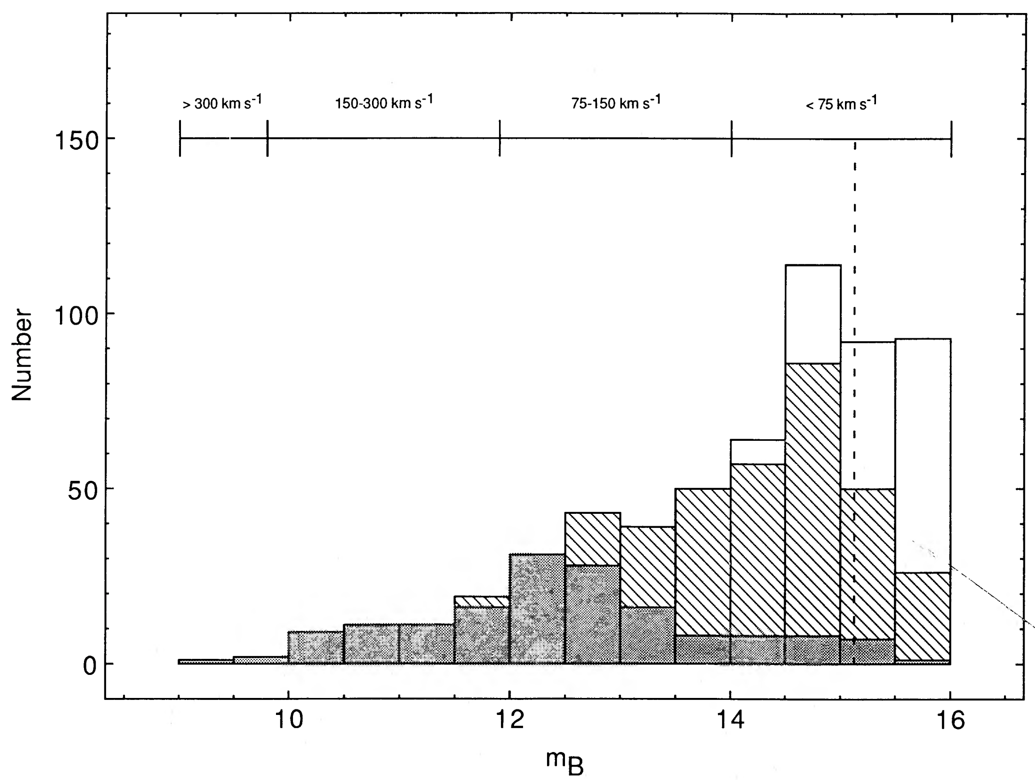

FIG. 13.—Relative completeness of various Virgo Cluster samples. Total area: apparent magnitude distribution of all galaxies deemed probable cluster members by Binggeli, Sandage, and Tammann (1985). *Hatched area*: subset with velocities confirming cluster membership. *Dark shaded area*: subset contained in the *Nearby Galaxies Catalog*.

removing the effects of incompleteness can be attributed to the morphology–local density relation.)

The results presented in this paper provide no support for the idea of biased galaxy formation. Whether they represent a contradiction depends on the predictions of a particular biasing model and on how characteristic the results of our small sample are of the general galaxy population. Large-scale variations in the clustering properties of galaxies clearly exist (see Kirshner *et al.* 1989). However, if the biasing mechanism is local, one would suspect that the differential clustering properties of various classes of galaxies within a volume would vary less than the overall amplitude of the clustering. Nonlocal biasing mechanisms, on the other hand, could give rise to such large-scale variations. In any case, it is clear that more data, covering larger volumes of the universe, are needed to obtain a definitive result. The recently completed 21 cm redshift survey of all 1849 UGC dwarf irregulars by Thuan (1988) should be very useful for this.

If the dwarf irregulars studied here are representative of galaxies with low internal velocities, our data do not appear to be consistent with the predictions of the models of White *et al.* (1987) and Dekel and Silk (1986). White *et al.* (1987) have calculated the effect of a biasing which occurs naturally in their CDM model on the correlation function of different mass galaxies. They find that, at scales of a few megaparsecs, the autocorrelation function of objects with circular velocities greater than 250 km s^{-1} is higher than that of all objects with circular velocities greater than 100 km s^{-1} by a factor of 2.2. This ratio of circular velocities is somewhat smaller than that in our two samples. The mean velocity width of the GH galaxies is larger than that of the entire dwarf sample by a factor of 2.4, and larger than that of the sample of dwarfs with $\delta v < 100$ km s^{-1} by a factor of 3.4. It is clear, from inspection of Figure 11, that a difference in amplitude of 2.2 is not consistent with any of the cross-correlation or autocorrelation functions which we have determined.

Perhaps the idea of dwarfs being more smoothly distributed is wrong, or perhaps the effect, as predicted by the theory of Dekel and Silk, can only be seen in the distribution of gas-poor dwarfs. However, the extant data strongly suggest that gas-poor dwarfs are even more strongly clustered than are the gas-rich ones (Binggeli 1988). There are other classes of objects which do appear to have smoother distributions in the neighborhood of voids. A number of emission-line galaxies have been discovered within the Bootes void (Moody *et al.* 1987); and Lyman-α absorbing clouds along the lines of sight toward QSOs are known to be much less clustered than are galaxies (Sargent *et al.* 1980). However, there is no reason to suppose that these classes of objects are more reliable tracers of the underlying mass distribution. They might be objects whose formation rate is much enhanced in low-density environments.

Which of the formation scenarios currently under discussion do predict voids empty of all visible galaxies, independent of type? Long-range biasing in CDM, where radiation or fast particles from early galaxies suppress the formation of galaxies in large regions far away (Rees 1985; Dekel and Rees 1987), could affect all types of galaxies equally. The baryonic scenarios, which assume an open universe (Blumenthal, Dekel, and Primack 1988), try to avoid the issue of biasing altogether. They do predict large regions of low density, but not as low as indicated by the galaxy voids, because the growth of fluctuations freezes out in an open model. In this respect, they do not do better than the $\Omega = 1$ biased CDM model. The neutrino-dominated scenario assumes that galaxies form only in pancakes, and hence it predicts $30h^{-1}$ Mpc volumes empty of all types of galaxies, in apparent agreement with our finding. As a matter of fact, this scenario suffers from the opposite problem: galaxy formation must be antibiased in high-density regions to be compatible with the observed clustering pattern (White, Frenk, and Davis 1983; Braun, Dekel, and Shapiro 1988). Among non-Gaussian models, the explosion scenario (Ostriker and Cowie 1981; Ikeuchi 1981) predicts substantial evacuation of gas from large regions, resulting in voids completely empty of galaxies.

We wish to thank Riccardo Giovanelli and Martha Haynes for giving us access to their unpublished data, Murray Lewis for guiding us through our radio observing, and Phil Perillat for help with the equipment. The Second Palomar Sky Survey is being undertaken on the Oschin 48 inch (1.2 m) Schmidt Telescope with primary funding by the National Geographic Society and Eastman Kodak, and additional funding from the Alfred P. Sloan Foundation and National Science Foundation grant AST84-16704. The work in this paper was partially supported by National Science Foundation grant AST81-19986. J. E. gratefully acknowledges support by an Amelia Earhart Fellowship during part of the course of this work.

REFERENCES

Abell, G. O. 1965, *Ann. Rev. Astr. Ap.*, **3**, 1.
Bicay, M. D., and Giovanelli, R. 1986, *A.J.*, **91**, 705.
Binggeli, B. 1988, preprint.
Binggeli, B., Sandage, A., and Tammann, G. 1985, *A.J.*, **90**, 1681 (BST).
Binggeli, B., Tarenghi, M., and Sandage, A. 1988, in preparation.
Blumenthal, G. R., Dekel, A., and Primack, J. R. 1988, *Ap. J.*, **326**, 539.
Bothun, G. D., Beers, T. C., Mould, J. R., and Huchra, J. P. 1986, *Ap. J.*, **308**, 510.
Braun, E., Dekel, A., and Shapiro, P. 1988, *Ap. J.*, **328**, 34.
Bridle, A. H., Davis, M. M., Fomalont, E. R., and Lequeux, J. 1972, *A.J.*, **77**, 405.
Davis, M., and Djorgovski, S. 1985, *Ap. J.*, **299**, 15.
Davis, M., and Geller, M. J. 1976, *Ap. J.*, **208**, 13.
Davis, M., and Huchra, J. P. 1982, *Ap. J.*, **254**, 437.
Davis, M., Huchra, J. P., Latham, D., and Tonry, J. 1982, *Ap. J.*, **253**, 423.
Davis, M., and Peebles, P. J. E. 1983, *Ap. J.*, **267**, 465.
Dekel, A., and Rees, M. J. 1987, *Nature*, **326**, 455.
Dekel, A., and Silk, J. 1986, *Ap. J.*, **303**, 39.
de Vaucouleurs, G., de Vaucouleurs, A., and Corwin, H. C. 1976, *Second Reference Catalogue of Bright Galaxies* (Austin: University of Texas Press).
Dressler, A. 1980, *Ap. J.*, **236**, 351.
Eder, J., and Oemler, A. 1989, in preparation.
Fisher, J. R., and Tully, R. B. 1975, *Astr. Ap.*, **44**, 151.
Giovanelli, R., and Haynes, M. P. 1985, *A.J.*, **90**, 2445.
———. 1988, in preparation.
Giovanelli, R., Haynes, M. P., and Chincarini, G. L. 1986, *Ap. J.*, **300**, 77 (GHC).
Giovanelli, R., Haynes, M. P., Meyers, S. T., and Roth, J. 1986, *A.J.*, **92**, 250.
Haynes, M. P., and Giovanelli, R. 1984, *A.J.*, **89**, 758.
Hoffman, G. L., Helou, G., Salpeter, E. E., Glosson, J., and Sandage, A. 1987, *Ap. J. Suppl.*, **63**, 247.
Ikeuchi, S. 1981, *Pub. Astr. Soc. Japan*, **33**, 221.
Kaiser, N. 1984, *Ap. J. (Letters)*, **284**, L9.
Kirshner, R. P., Oemler, A., and Schechter, P. L. 1979, *A.J.*, **84**, 951 (KOS).
Kirshner, R. P., Oemler, A., Schechter, P. L., and Shectman, S. A., 1981, *Ap. J. (Letters)*, **248**, L57.

Kirshner, R. P., Oemler, A., Schechter, P. L., and Shectman, S. A. 1987, *Ap. J.*, **314**, 493.
———. 1989, in preparation.
Kuhr, H., Witzel, A., Pauliny-Toth, I. I. K., and Nauber, U. 1981, *Astr. Ap. Suppl.*, **45**, 367.
Lewis, B. M., Helou, G., and Salpeter, E. E. 1985, *Ap. J. Suppl.*, **59**, 161.
Moody, J. W., Kirshner, R. P., MacAlpine, G. M., and Gregory, S. A. 1987, *Ap. J.* (*Letters*), **314**, L33.
Nilson, P. 1973, *Uppsala General Catalogue of Galaxies* (*Uppsala Astr. Obs. Ann.*, Vol. **6**) (UGC).
Oemler, A. 1974, *Ap. J.*, **194**, 1.
———. 1988, in *A.S.P. Conf. Proc.*, Vol. **3**, *Galaxy Clustering and Large Scale Structure*, ed. J. M. Dickey.
Ostriker, J. P., and Cowie, L. L. 1981, *Ap. J.* (*Letters*), **243**, L127.
Phillips, S., and Shanks, T. 1987, *M.N.R.A.S.*, **229**, 621.
Rees, M. J. 1985, *M.N.R.A.S.*, **213**, 75.
Sargent, W. L. W., Young, P. J., Boksenberg, A., and Tytler, D. 1980, *Ap. J. Suppl.*, **42**, 41.
Schombert, J., and Bothun, G. D. 1988, *A.J.*, **95**, 1389.
Sharp, N. A., Jones, B. J. T., and Jones, J. E. 1978, *M.N.R.A.S.*, **185**, 457 (SJJ).
Thuan, T. X. 1988, in *Proc. 1988 Moriond Workshop on Dark Matter*, ed. J. Audouze (Gif sur Yvette: Editions Frontières).
Thuan, T. X., Gott, J. R., and Schneider, S. E. 1987, *Ap. J.* (*Letters*), **315**, L93.
Tully, R. B. 1988, *Nearby Galaxies Catalog* (Cambridge: Cambridge University Press).
White, S. D. M., Davis, M., Efstathiou, G., and Frenk, C. S. 1987, *Nature*, **330**, 451.
White, S. D. M., Frenk, C. S., and Davis, M. 1983, *Ap. J.* (*Letters*), **274**, L1.
White, S. D. M., Tully, R. B., and Davis, M. 1988, *Ap. J.* (*Letters*), **333**, L45 (WTD).
Zwicky, F., Herzog, E., Karpowicz, M., Kowal, C. T., and Wild, P. 1961–1968, *Catalog of Galaxies and Clusters of Galaxies* (Pasadena: California Institute of Technology) (CGCG).

AVISHAI DEKEL: Racah Institute of Physics, Hebrew University, Jerusalem, Israel

JO ANN EDER and AUGUSTUS OEMLER, JR.: Yale University Observatory, P.O. Box 6666, New Haven, CT 06511

JAMES M. SCHOMBERT: Robinson Laboratory, California Institute of Technology, Pasadena, CA 91125